Lab Notes

Editors
Thomas M. Moses | Shane F. McClure

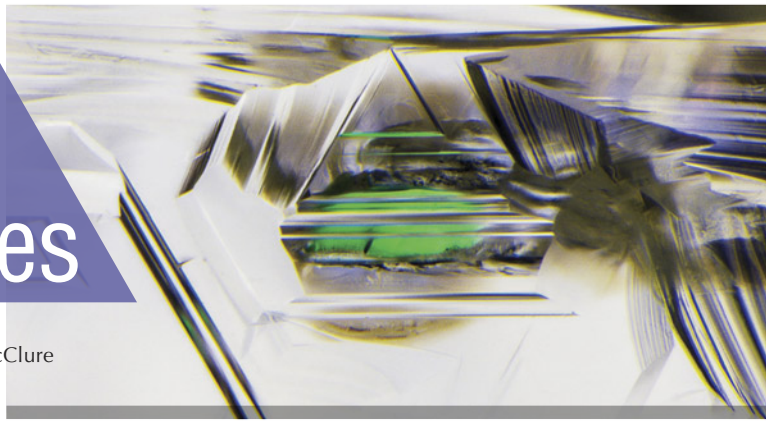

DIAMOND

Exceptional Natural-Color Fancy Red Diamond

The Carlsbad laboratory recently received a 1.21 ct Fancy orangy red round brilliant cut diamond (6.62–6.84 × 4.14 mm; figure 1) for a colored diamond grading and identification report. Results of standard gemological testing and microscopic observation confirmed it had a natural color and no color treatment or clarity enhancement. The stone displayed faint fluorescence under long-wave UV and none under short-wave UV. Fourier-transform infrared spectroscopy indicated a type IaB diamond, while ultraviolet/visible (550 nm band and H3 [503.2 nm] center) and photoluminescence (PL) spectroscopy indicated natural color without any treatment. The 550 nm absorption band is closely linked to plastic deformation, which is clearly reflected in the broad emission features in the PL results. Due to the extensive plastic deformation, some fractures could have developed.

The rarity and high value of red diamonds has resulted in many attempts to reproduce this color through treatment or even laboratory growth procedures with post-growth treatment (S. Eaton-Magaña and J.E. Shigley, "Observations on CVD-grown synthetic diamonds: A review," Fall 2016 *G&G*, pp. 222–245; S. Eaton-Magaña and J.E. Shigley, "Observations on HPHT-grown synthetic diamonds: A review," Fall 2017 *G&G*, pp. 262–284). However, treated red diamonds are often accompanied by purplish or brownish color components that are not desirable and are different from the purer hues of naturally red diamonds (W. Wang et al., "Treated-color pink-to-red diamonds from Lucent Diamonds Inc.," Spring *G&G* 2005, pp. 6–19). Natural-color red diamonds are so rare that only around a couple dozen true red diamonds are known to exist, and most of these are under half a carat.

The exceptional natural-color 1.21 ct Fancy orangy red diamond examined here is a fine example of natural-color red diamond. It has yet to be named.

Maryam Mastery Salimi

Figure 1. This 1.21 ct round brilliant diamond is notable for its size and natural Fancy orangy red color.

Treated "Nickel-Rich" Green Diamond

Natural-color green diamonds are extremely rare. The cause of color for most green diamonds is attributed primarily to radiation damage resulting from exposure to radioactive elements over geologic time (W. Wang et al., "Natural type Ia diamond with green-yellow color due to Ni-related defects," Fall 2007 *G&G*, pp. 240–243). The New York laboratory recently received a 2.12 ct pear-shaped diamond measuring 9.52 × 7.24 × 4.27 mm that was graded as Fancy yellow-green (figure 2), and testing attributed the color to several mechanisms.

Figure 2. This 2.12 ct Fancy yellow-green diamond owes its color to both the nickel-related absorption band and the artificially introduced GR1 absorption.

Editors' note: All items were written by staff members of GIA laboratories.

Gems & Gemology, Vol. 58, No. 3, pp. 354–363.

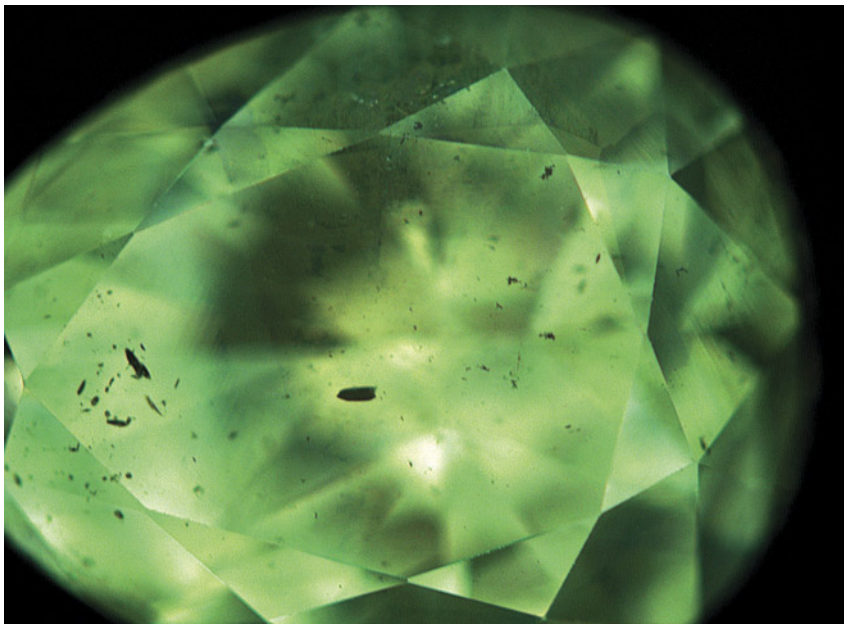

Figure 3. DiamondView imaging reveals greenish yellow fluorescence that is typical for nickel-rich diamond.

Microscopic examination revealed dark crystals and clouds throughout the stone, and infrared spectroscopy confirmed it was a type Ia diamond. DiamondView imaging showed greenish yellow fluorescence (figure 3), typical for "nickel-rich" diamond.

Figure 4. UV-Vis-NIR spectra show the nickel-related absorption band and 883 peak in both a natural diamond from the GIA database and the 2.12 ct treated diamond. In addition, the spectrum for the treated diamond shows the GR1 peak around 740 nm. Spectra are offset vertically for clarity.

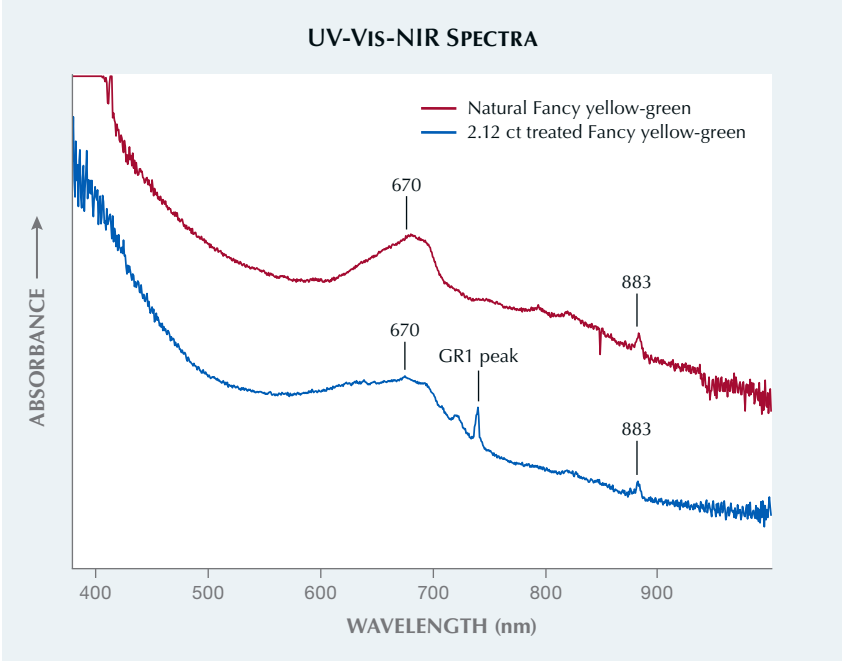

The ultraviolet/visible/near-infrared (UV-Vis-NIR) absorption spectrum showed a nickel-related absorption band at around 670 nm, a peak at 883 nm (an attributed peak in "nickel-rich" diamonds), and a GR1 (general radiation damage) peak at about 740 nm (figure 4). This is an uncommon combination of spectral features in diamond. The Ni-related absorption band is usually responsible for the green color in this type of diamond (Fall 2013 Lab Notes, pp. 173–174; Spring 2022 Lab Notes, pp. 50–51). In this particular diamond, the yellow-green color saturation can be attributed to both the nickel-related absorption band and the GR1 absorption. We have not observed these two features together in natural-color green diamond. Additional testing and gemological observations confirmed that the GR1 peak was artificially introduced, and we concluded that the color was treated. The color was likely a lighter and less saturated green before treatment.

This stone illustrates the importance of combining gemological observations with spectroscopic characteristics to separate natural- and treated-color green diamonds.

Luthfia Syarbaini and Paul Johnson

Gota de Aceite–Like Effect in a Brazilian EMERALD

Internal optical effects can provide useful information to help identify gemstones and understand their nature and geographic origin. For example, *gota de aceite*, a roiled or "drop of oil" appearance seen in Colombian emeralds, is considered to be caused by irregularities in the crystal structure due to rapid growth triggered by alteration of the growth conditions (e.g., R. Ringsrud, "*Gota de aceite*: Nomenclature for the finest Colombian emeralds," Fall 2008 *G&G*, pp. 242–245; Winter 2017 Lab Notes, pp. 460–461).

Recently, GIA's Tokyo laboratory examined a 2.99 ct step-cut emerald measuring 10.17 × 8.12 × 5.50 mm (figure 5) for geographic origin determination. This stone exhibited a unique

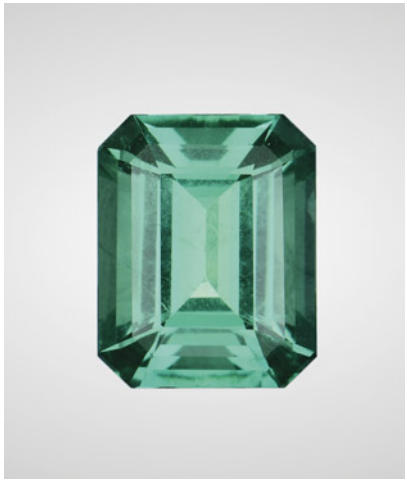

Figure 5. This 2.99 ct Brazilian emerald displayed a roiled effect similar to the gota de aceite *phenomenon.*

roiled growth structure resembling the *gota de aceite* effect (figure 6, left) at an angle nearly perpendicular to the table facet. The *gota de aceite* structure was visible parallel to the *c*-axis of the emerald based on microscopic and polariscopic observations. From other directions such as girdle to girdle, the effect was not visible and columnar growth structure was observed. The emerald also contained numerous reflective raindrop-like needles and tubes (figure 6, right) and irregular two-phase inclusions. This stone had a refractive index range of 1.580–1.588 and showed no reaction under a Chelsea color filter. The ultraviolet/visible/near-infrared spectrum showed a significant Fe^{2+} broad band at around 810 nm. These internal and standard gemological features did not match Colombian origin, with the exception of the *gota de aceite* effect. Laser ablation–inductively coupled plasma–mass spectroscopy revealed a high iron concentration (4540–4800 ppmw) and medium potassium (230–254 ppmw) and lithium (62–68 ppmw) contents. A Brazilian origin was determined based on inclusions and trace element composition (S. Saeseaw et al., "Geographic origin determination of emerald," Winter 2019 *G&G*, pp. 614–646).

The *gota de aceite* optical phenomenon has been used as a characteristic feature of classic Colombian emeralds, but a similar pattern was previously reported in a Zambian emerald (Winter 2017 Lab Notes, pp. 460–461). The similarity in the growth pattern suggests that the growth conditions causing the rapid emerald crystallization were similar, although the geological origins and chemical compositions of both emeralds are different. As several microscopic studies on emerald have concluded (e.g., S. Saeseaw et al., "Three-phase inclusions in emerald and their impact on origin determination," Summer 2014 *G&G*, pp. 114–132; Winter 2017 Lab Notes, pp. 460–461), inclusions and internal features may not always be helpful in determining geographic origin, and the *gota de aceite* effect may not offer enough evidence for Colombian origin. Careful observation of other inclusions combined with advanced testing is required for origin determination of emerald.

Makoto Miura

Treated Orange and Pink CVD LABORATORY-GROWN DIAMOND

Recently, GIA received two similarly treated diamonds grown by chemical vapor deposition (CVD): a 2.00 ct Fancy Deep orange and a 3.00 ct Fancy Vivid orangy pink (figure 7). A database search revealed that the Fancy Deep orange was the first CVD-grown diamond with an unmodified orange color ever submitted to GIA. CVD-grown diamonds with an orangy pink color are far more common, and the 3.00 ct sample provided for an interesting comparison. From examination of the visible/near-infrared

Figure 6. Internal features observed in the 2.99 ct Brazilian emerald. Left: Gota de aceite*–like optical effect with columns resembling drops of oil. Note that this image was taken at an angle parallel to the* c*-axis. Right: Numerous raindrop-like needles and tubes. Fields of view 3.10 and 2.46 mm.*

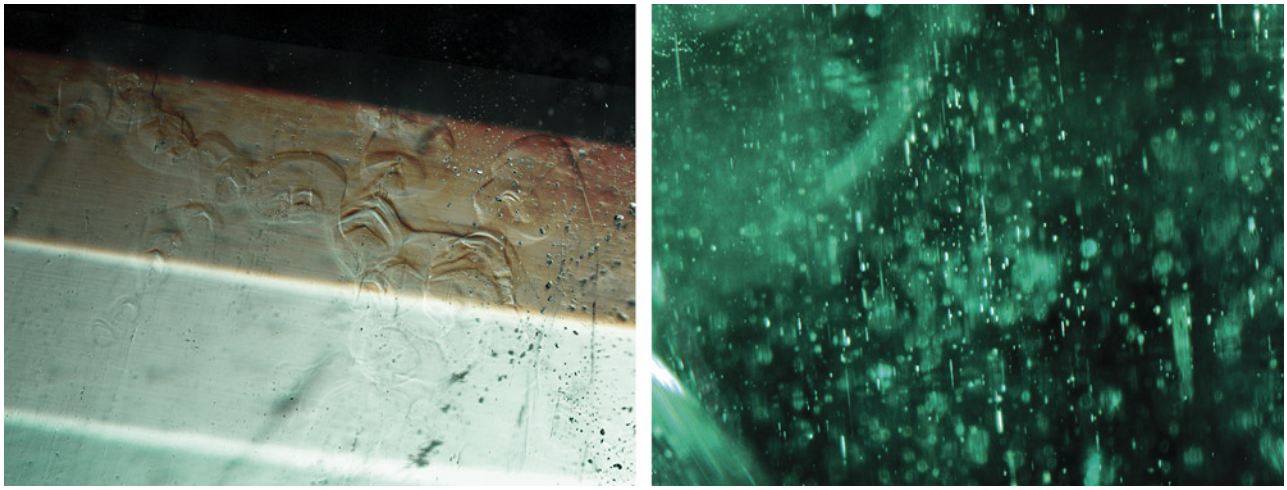

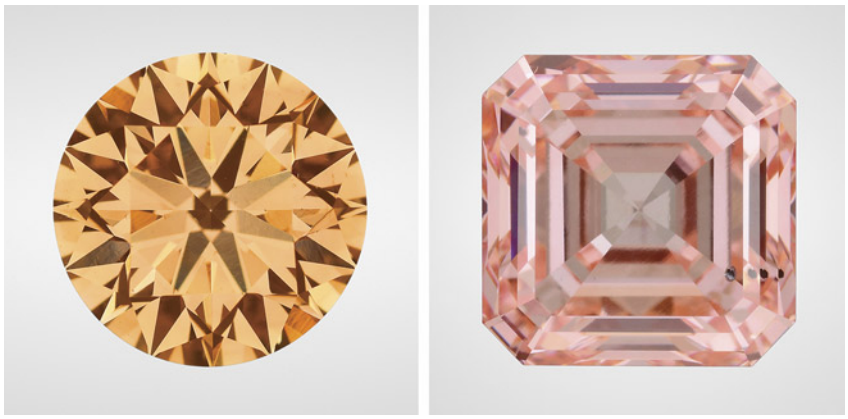

Figure 7. These 2.00 ct Fancy Deep orange (left) and 3.00 ct Fancy Vivid orangy pink (right) CVD-grown diamonds were subjected to multiple treatments including HPHT processing, irradiation, and low-temperature annealing to achieve the final color grades.

(Vis-NIR) absorption spectra, both samples had similar features and likely underwent similar treatment processes (figure 8). The subtle differences in relative peak intensities were sufficient to create the distinctly different appearances and color grades.

The Vis-NIR absorption spectra for both CVD-grown diamonds showed nitrogen vacancy centers (principal absorption for NV^0 at 575 nm and NV^- at 637 nm), 594 nm peak, and the GR1 center. Both samples also displayed strong absorption of the SiV^- center (737 nm). In the Fancy Deep orange sample, the NV centers exhibited lower absorption than in the orangy pink sample and also a slightly greater SiV^--related absorption, which helped shift the transmission window from the red (i.e., pink) toward the orange.

Figure 8. The 2.00 ct Fancy Deep orange and the 3.00 ct Fancy Vivid orangy pink CVD-grown diamonds underwent similar post-growth treatments and show similar defect centers in their Vis-NIR absorption spectra, including the NV centers, 594 nm, SiV^-, and GR1. However, subtle differences in relative defect concentrations lead to their distinct color appearances. Although very small, the GR1 defect was also detected in the absorption spectrum of the 2.00 ct CVD-grown diamond. Spectra are offset vertically for clarity.

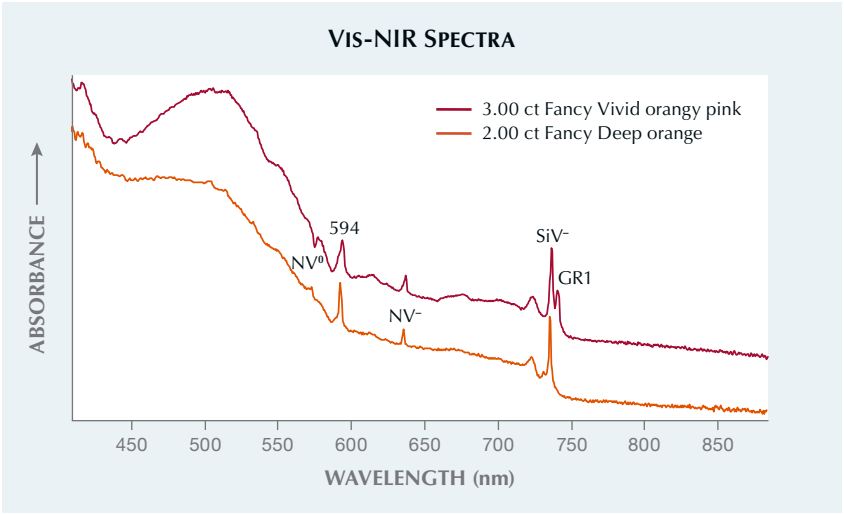

Based on the comparatively low value of the 468 nm emission peak determined by 457 nm photoluminescence spectroscopy, both CVD-grown diamonds showed evidence of high-pressure, high-temperature (HPHT) treatment; they were subsequently irradiated to generate the radiation-related features that included the 594 nm peak and the GR1 center. Irradiation was followed by low-temperature annealing, which was intended to generate additional NV centers without fully annihilating the GR1 center. The 594 nm center is a radiation-related defect in nitrogen-containing diamonds. In the IR absorption spectra of both CVD-grown diamonds, small peaks at 1344 cm^{-1} were observed. From those peaks, the single nitrogen concentration could be estimated as ~1 ppm (S. Eaton-Magaña and J.E. Shigley, "Observations on CVD-grown synthetic diamonds: A review," Fall 2016 *G&G*, pp. 222–245).

Both samples presented red fluorescence when excited by the deep UV wavelengths of the DiamondView, a feature that is consistent with the strong nitrogen-vacancy centers in these CVD-grown diamonds. However, neither sample showed any noticeable photochromic effects from the deep UV exposure, something that can occur in CVD-grown diamonds due to charge transfer of the NV centers or the SiV^- centers (S. Eaton-Magaña et al., "Laboratory-grown diamond: A gemological laboratory perspective," *Journal of Gems and Gemmology*, 2021, Vol. 23, No. 6, pp. 25–39).

The Fancy Deep orange sample was interesting to observe, as unmodified orange colors are extremely rare among natural diamonds and, until now, laboratory-grown samples. Subtle engineering of defect concentrations during post-growth treatment

Figure 9. The 1.72 ct yellowish brown and black non-nacreous (porcelaneous) pearl with Telescopium telescopium *shells provided by the client. The intact shell is approximately 70 × 35 mm and the sawn shell is approximately 84 × 41 mm. Inset: An enlarged image of the pearl.*

can lead to vastly different results in the color grades.

Sally Eaton-Magaña and Paul Johnson

A Non-Nacreous Pearl Reportedly from *Telescopium telescopium*

GIA's Bangkok laboratory recently examined a yellowish brown and black non-nacreous button-shape pearl weighing 1.72 ct and measuring 6.64 × 6.53 × 5.07 mm. The pearl exhibited an attractive porcelain-like luster.

The client informed GIA that the pearl was found in a *Telescopium telescopium* shell. This edible snail (N. George et al., "DNA barcoding of gastropod *Telescopium telescopium* (Linnaeus, 1758) found at the Karachi coast, Pakistan," *Journal of Animal and Plant Sciences*, Vol. 31, No. 5, 2021, pp. 1530–1536) was retrieved from an abandoned shrimp pond near a mangrove forest in Krabi, Thailand. The story of the pearl's discovery was widely publicized in the local media. Though the client was unable to submit the shell from which the pearl was extracted, they provided us with samples of the same type of shell for further study (figure 9).

Observation through a 10× loupe and a microscope revealed long cracks traversing the darker side of the pearl (figure 10A). No polishing lines or evidence of surface or color modification were observed, indicating that the shape and color were natural. The pearl and shells exhibited flame structures similar to those routinely observed in pearls such as those from the horse conch (Summer 2018 Lab Notes, pp. 211–212). Intersecting and overlapping flame structures typically observed in pearls from the *Cassis* genus (Fall 2012 Lab Notes, pp. 211–212) were also detected on the pearl (figure 10B) and shells (figure 10C). However, the banded structure observed on the cut shells (figure 10D) was not visible on the pearl, additional evidence that the client's item was a pearl and not an imitation fashioned from shell.

Real-time microradiography confirmed a natural whole pearl, as growth arcs close to the center and surface-reaching cracks were revealed (figure 11). As expected, energy-dispersive X-ray fluorescence analysis detected calcium as a major component in the pearl and shells, while manganese levels of less than 15 ppm and strontium levels ranging from 1005 to 2675 ppm verified a saltwater

Figure 10. A: Obvious long cracks traversing the pearl's darker side; field of view 7.20 mm. B: Intersecting flame structure on the pearl; field of view 2.40 mm. C: Intersecting flame structure on a cross section of the shell; field of view 4.80 mm. D: Banding and flame structure on a cut area of shell; field of view 4.80 mm.

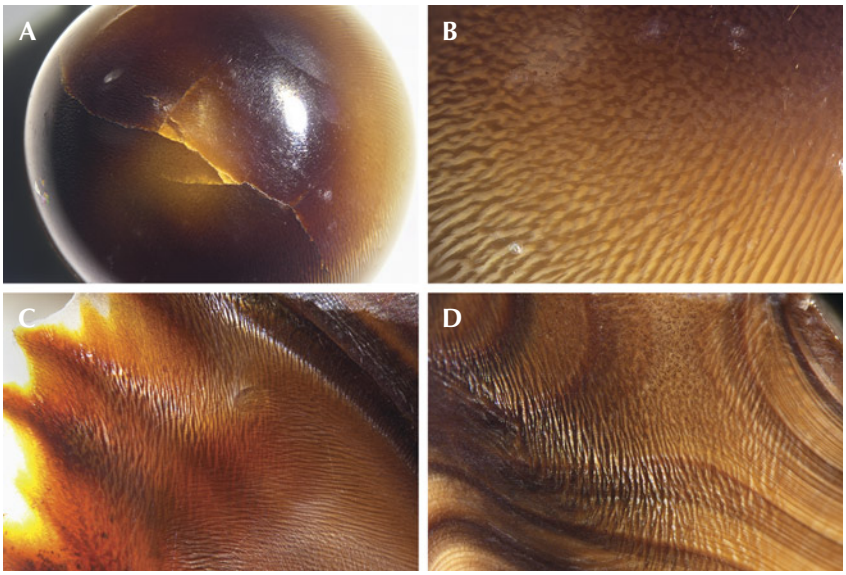

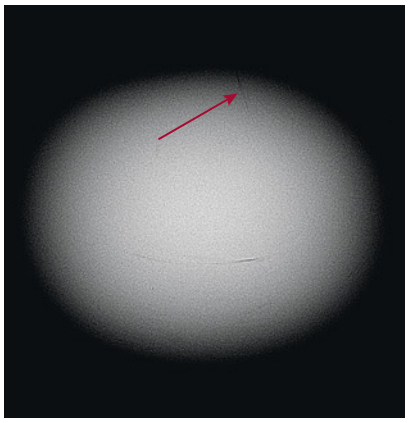

Figure 11. Real-time microradiography revealed growth arcs close to the center and surface-reaching cracks (red arrow).

formation environment. The pearl's natural color was substantiated using additional advanced spectroscopic methods. Raman spectra collected using a 514 nm argon ion laser on the pearl and shells (figure 12) revealed peaks related to the vibration modes of aragonite at 703, 1085, and 1464 cm^{-1}; polyenic-related peaks at 1017, 1105–1120, 1297, and 1490–1500 cm^{-1} (S. Karampelas et al., "Polyacetylenic pigments found in pearls and corals," *30th International Gemmological Conference*, Moscow, 2007; L. Bergamonti et al., "The nature of the pigments in corals and pearls: A contribution from Raman spectroscopy," *Spectroscopy Letters*, Vol. 44, No. 7-8, 2011, pp. 453–458); and an additional peak at 1175 cm^{-1} that is also likely related to polyene.

Surface observations and data collected from the pearl and shells using analytical methods appeared to support the claim that the pearl formed in this mollusk species. However, this can only be confirmed by conducting DNA barcoding analysis, which is a destructive test. This report adds to the growing list of natural pearls found in edible oysters and snails described in the literature (e.g., Winter 1995 Gem News, pp. 280–281; K. Scarratt et al., "A note on a pearl attached to the interior of *Crassostrea virginica* (Gmelin, 1791) (an edible oyster, common names, American or Eastern oyster)," *Journal of Gemmology*, Vol. 30, No. 1-2, 2006, pp. 43–50; Fall 2019 Gem News International, pp. 439–440; Fall 2020 Lab Notes, pp. 420–422; Summer 2021 Lab Notes, pp. 152–153). However, this is the first time a natural pearl has reportedly been discovered in a *Telescopium* species. Its unique appearance and characteristics provided a rare opportunity for GIA gemologists to examine and record data from a natural pearl originating from this marine snail.

Areeya Manustrong, Kwanreun Lawanwong, Ravenya Atchalak, and Nanthaporn Nilpetploy

Rare Kashmir Star SAPPHIRE

A rare star sapphire of Kashmir origin, mounted in a combination ring and pendant (figure 13), was recently examined in the New York laboratory. Kashmir has long been regarded as the

Figure 12. Raman spectra of the pearl and a shell obtained using a 514 nm argon ion laser revealed peaks related to the vibration modes of aragonite at 703, 1085, and 1464 cm^{-1} (obscured by stacking); polyenic-related peaks at 1015, 1120, 1296, and 1493 cm^{-1}; and an additional peak at 1175 cm^{-1} that is also likely related to polyene. Spectra are offset vertically for clarity.

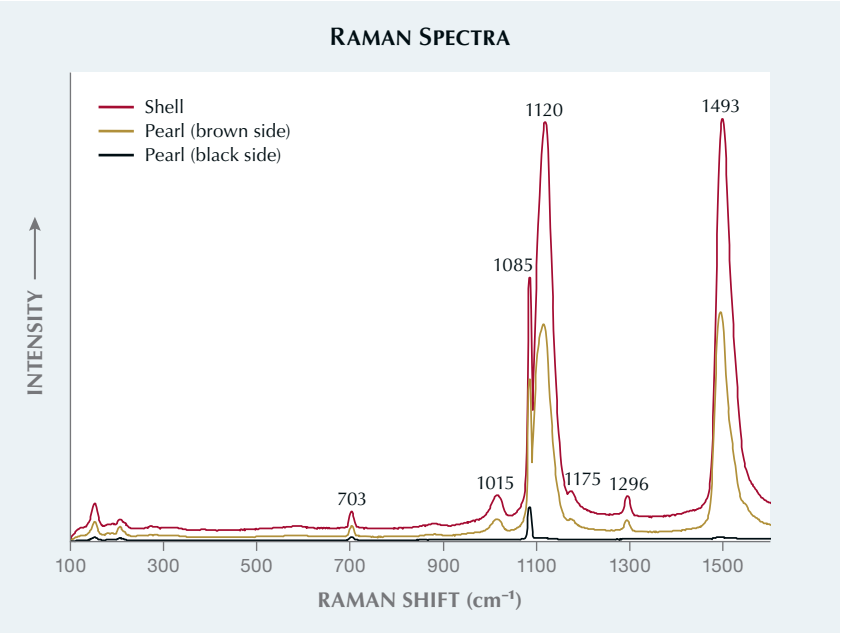

Figure 13. An approximately 15 ct blue Kashmir star sapphire set in a combination ring and pendant with near-colorless pear and marquise brilliants.

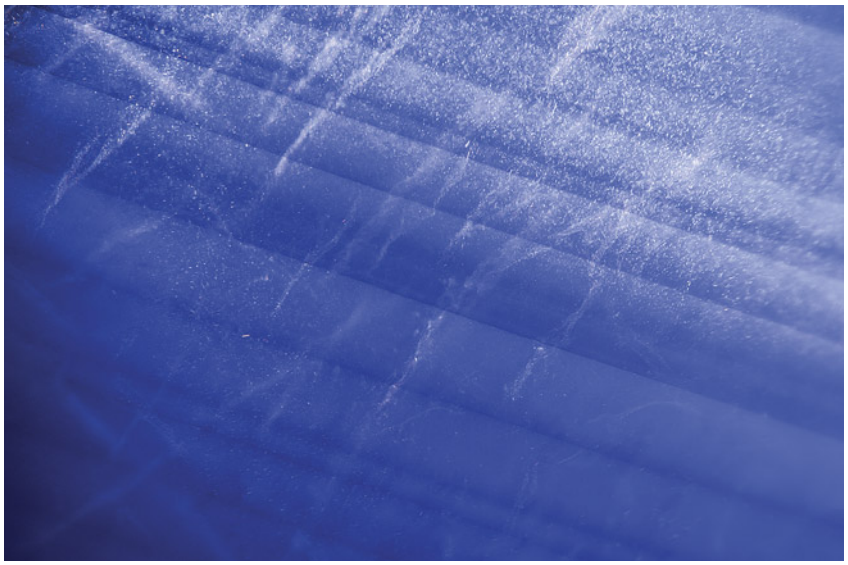

Figure 14. Wispy stringers among sharp milky bands of microscopic particles. Field of view 3.57 mm.

most sought-after source of blue sapphire since the deposit's discovery in the late nineteenth century. Words such as "sleepy" or "velvety" are often used to describe their characteristic appearance, which can be attributed to the scattering of light as it interacts with "milky" bands of microscopic particles within the stone. Due to the locality's limited production, Kashmir sapphires are scarce in the market, and star sapphires are particularly uncommon (R.W. Hughes et al., *Ruby & Sapphire: A Gemologist's Guide*, 2017, RWH Publishing/Lotus Publishing, Bangkok, p. 477).

This blue cabochon star sapphire was estimated to weigh around 15 ct. A spot reading gave an approximate refractive index of 1.76, matching corundum. Microscopic inspection revealed sharp, angular milky bands and particle streamers (figure 14), both features that are typical of Kashmir sapphires. Several sparse short silk needles were also observed (figure 15). Asterism in corundum is generally caused by the reflection of light off of exsolution rutile silk needles. This sapphire's star, however, was generated by light reflected from the crystallographically oriented bands of minute particles.

Further testing of the sapphire's spectral and chemical properties was carried out to help determine its geographic origin. Laser ablation–inductively coupled plasma–mass spectrometry revealed a trace element chemistry consistent with stones of known Kashmir origin, based on GIA's internal reference data. This, coupled with the material's internal characteristics, confirmed that the star sapphire was in fact from Kashmir. No evidence of heat treatment was detected. While the majority of corundum on the market is heated to improve color, high-quality sapphires from Kashmir are generally left untreated.

Kashmir sapphires are rare enough in their own right. Furthermore, a large star sapphire from this historic locality is truly an extraordinary sight, and certainly a first for the author.

Emily Jones

SYNTHETIC MOISSANITE

Fraudulently Inscribed Synthetic Moissanite

Stones with fraudulent GIA inscriptions are frequently reported. To verify diamond identity, GIA recently announced a diamond matching service using GIA Match iD, based on laser inscription imaging. In most cases of fraud, the inscribed material is diamond (Fall 2017 Lab Notes, p. 366), but there has also been a report involving non-diamond materials (Fall 2020 Lab Notes, pp. 424–425). A similar case was recently identified.

The Mumbai laboratory received a 1.71 ct square modified brilliant (figure

Figure 15. Several short needles of exsolution silk amid the abundant particle stringers. Field of view 1.85 mm.

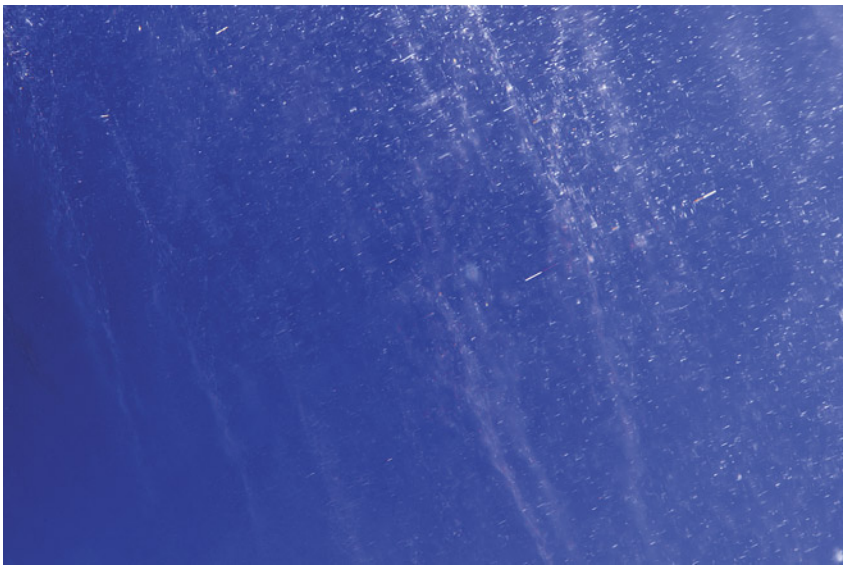

Figure 16. This 1.71 ct square modified brilliant bears a fraudulent GIA inscription.

16) for update service. The girdle was inscribed with "GIA" and a number matching an existent report, although the font was different from that of an actual GIA inscription (figure 17). The inscribed report number matched one for a natural diamond, a 1.71 ct square modified brilliant cut. Compared with a typical laser inscription from the GIA laboratory, this one was significantly different. Gemological and spectroscopic examination confirmed that the brilliant was synthetic moissanite. In addition to diamonds and synthetic moissanite, GIA has previously identified laser inscriptions on cubic zirconia, diaspore, emerald, garnet, ruby, sapphire, spinel, tanzanite, and other materials.

Shoko Odake

Figure 17. The fraudulent inscription on the synthetic moissanite.

A Synthetic Moissanite Presented As Natural Diamond Rough

A 7.42 ct light bluish green specimen (figure 18) submitted to the New York lab for a colored diamond identification and origin report was identified as a synthetic moissanite crystal carved to resemble a natural diamond rough. Since synthetic moissanite resembles diamond at a glance and has a similar specific gravity and "heft," it could easily be mistaken for natural diamond. The sample was first identified as synthetic moissanite using Fourier-transform infrared (FTIR) spectroscopy (figure 19). The resulting data displayed a distinctive moissanite spectrum, with peaks occurring at 2079, 2297, and 2392 cm^{-1} (A.M. Hofmeister et al., "Optical constants of silicon carbide for astrophysical applications," *Astrophysical Journal*, Vol. 696, No. 2, 2009, pp. 1502–1516). This finding was confirmed with an analysis of the Raman spectrum, which showed strong 767, 788, and 798 cm^{-1} peaks, also consistent with synthetic moissanite (figure 20). Although natural moissanite does exist, crystals are tiny and fragmented. Gem-quality specimens have not yet been found (Summer 2014 Gem News International, pp. 160–161).

Figure 18. This 7.42 ct light bluish green synthetic moissanite, submitted as a diamond, displays triangular features on each of the octahedral faces.

Figure 19. The peaks at 2079, 2297, and 2392 cm^{-1} displayed in this FTIR spectrum are consistent with synthetic moissanite.

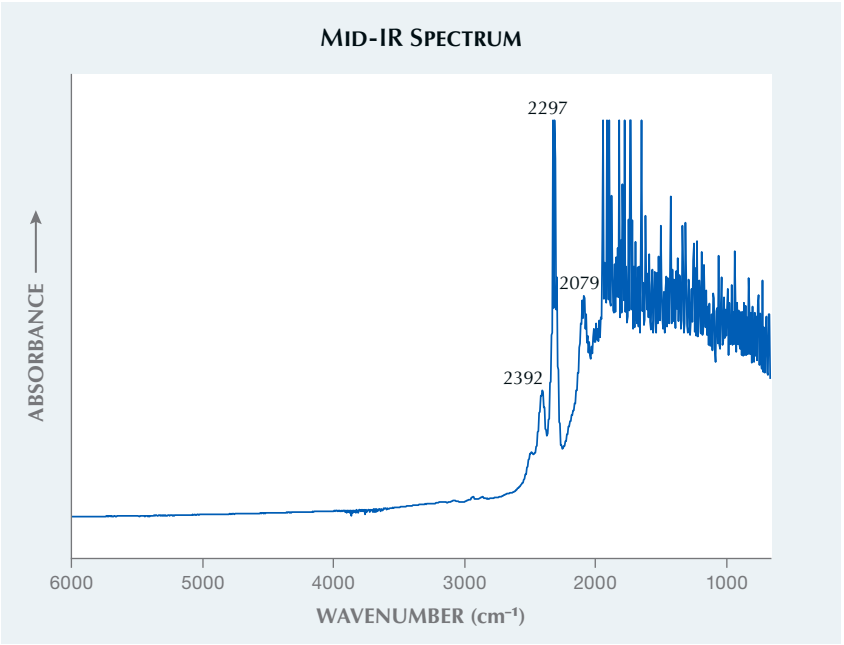

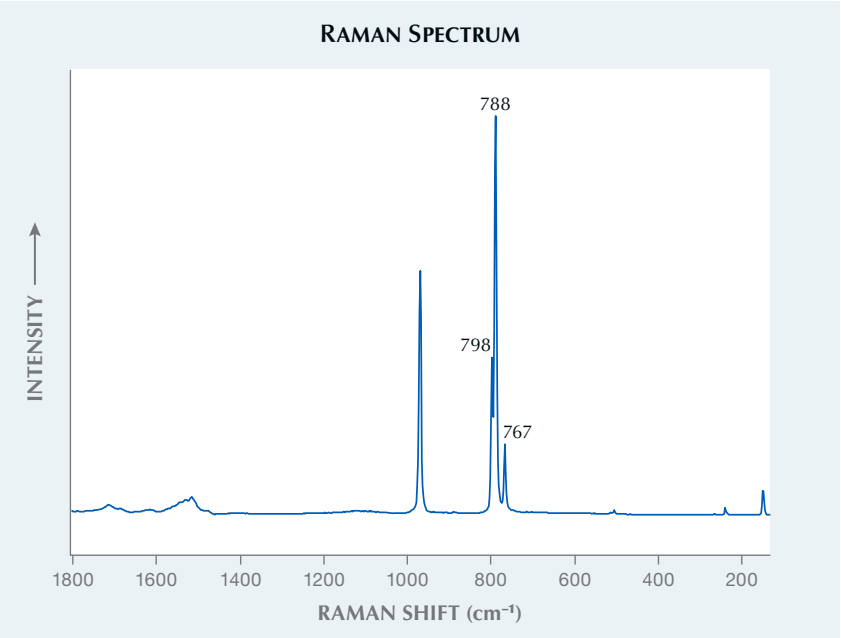

Figure 20. Raman spectroscopy confirmed the identification as synthetic moissanite, with peaks at 767, 788, and 798 cm^{-1}. (The sharp peak at 970 cm^{-1} suggests a hexagonal 6H type of silicon carbide.)

Figure 21. Exposure to kimberlitic fluids rich in O_2 and H_2O creates varied shapes and textures in natural diamond octahedra. This natural green diamond, known as the "Matryoshka" (Spring 2020 Lab Notes, pp. 127–129) has resorbed points and edges as well as trigonal etching on the {111} faces.

The turbid and stained 7.42 ct synthetic moissanite was shaped into a slightly rounded octahedron with prominent stepped edges. Octahedra belong to the cubic crystal class; both natural and synthetic SiC belong to the trigonal class and always display hexagonal prismatic to tabular forms. It was concluded that the synthetic moissanite rough had been carved into an octahedron, and that the detailing of the stepped edges and coarse textures were specifically chosen to imitate the appearance of a natural diamond octahedron that had been partially resorbed by kimberlitic magma, such as the natural diamond in figure 21. Although sharp and well-formed diamond octahedra are occasionally found preserved in mantle rocks entrained in kimberlitic eruptions, the vast majority of natural diamond crystals are exposed to corrosive kimberlitic fluids during their ascent through the cratonic mantle and display a wide variety of resorption textures (R. Tappert and M.C. Tappert, *Diamonds in Nature: A Guide to Rough Diamonds*, 2011, Springer Verlag, Heidelberg, Germany).

This investigation is a reminder to take caution when identifying gemstones, as intentional material processing steps such as these may be used to deceive consumers and could damage the integrity of the gem trade.

Courtney Robb and Sarah Arden

Cat's-Eye Paraíba TOURMALINE With Copper Inclusions

The Tokyo laboratory recently received a 1.33 ct greenish blue oval cabochon measuring 6.83 × 6.17 × 3.55 mm (figure 22) and displaying a cat's-eye effect. Standard gemological testing yielded a refractive index of 1.620–1.640, a uniaxial optical sign, and a hydrostatic specific gravity of 3.08, all consistent with tourmaline. Ultraviolet/visible/near-infrared spectrometry showed the absorption band at 900 nm, which is greater than the one at 700 nm, indicating the greenish blue color of this sample was dominated by copper (P.B. Merkel and C.M. Breeding, "Spectral differentiation between copper and iron colorants in gem tourmaline," Summer 2009 *G&G*, pp. 112–119). This stone meets the requirement for designation as a Paraíba tourmaline (Laboratory Manual Harmonisation Committee Information Sheet #6, 2012). Laser ablation–inductively coupled plasma–mass spectrometry indicated a high copper concentration of 11741–14794 ppmw. The high copper (over 10000 ppmw) is limited to Bra-

Figure 22. This 1.33 ct cat's-eye Paraíba tourmaline with copper inclusions shows a golden chatoyancy.

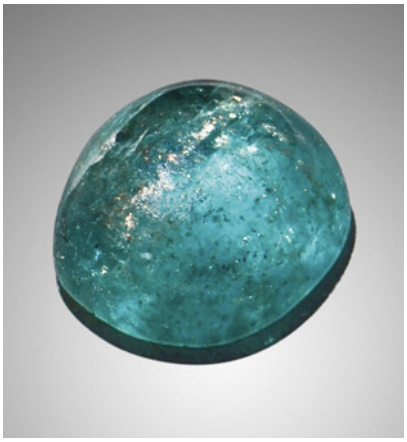

Figure 23. The copper inclusions on the lower right are partially reflecting light. Field of view 3.5 mm.

zilian origin (Y. Katsurada et al., "Geographic origin determination of Paraíba tourmaline," Winter 2019 *G&G*, pp. 648–659).

As previously reported (Winter 2018 Lab Notes, pp. 438–439), cat's-eye Paraíba tourmaline usually includes groups of parallel tube-like inclusions that create the phenomenon. However, that was not the case for this tourmaline.

Different from normal cat's-eye Paraíba tourmaline, the band of reflected light in this stone was stronger, with metallic luster. Microscopic examination revealed a fluid inclusion network, rounded metallic inclusions, and growth tubes, with many golden-colored dendritic inclusions causing the cat's-eye effect (figures 23 and 24). Raman spectroscopy could not be used to identify the inclusions, which were too thin and did not reach the surface. Such inclusions in Paraíba tourmaline have been reported and identified as natural copper (F. Brandstätter and G. Niedermayr, "Copper and tenorite inclusions in cuprian-elbaite tourmaline from Paraíba, Brazil," Fall 1994 *G&G*, pp. 178–183). The natural copper inclusions were aligned in the same direction, parallel to each other, and reflected the light to cause the chatoyant effect. This also explains why the reflective light band in this stone looked different from other cat's-eye Paraíba tourmaline.

While some cat's-eye Paraíba tourmalines have been examined in GIA laboratories, this is the first with chatoyancy caused by copper inclusions.

Yuxiao Li

PHOTO CREDITS
Diego Sanchez—1, 7 (left); Jian Xin (Jae) Liao—2, 18, 21; Luthfia Syarbaini—3; Shunsuke Nagai—5, 22; Makoto Miura—6; Sood Oil (Judy) Chia—7 (right); Lhapsin Nillapat and Nuttapol Kitdee—9; Ravenya Atchalak and Kwanreun Lawanwong—10, 11; Annie Haynes—13; Emily Jones—14, 15; Sushant Shinde—16; Sandesh Mali—17; Yuxiao Li—23, 24

Figure 24. The copper inclusions aligned in the same direction appear brownish and black (left) and together display golden luster when the light enters from a certain direction (right). Field of view 2.3 mm.